PROCEEDINGS OF SCIENCE

The optics and camera system of the Schwarzschild-Couder Telescope and the performance improvement to CTA

A. Acharyya,[1] C. B. Adams,[2] G. Ambrosi,[3] C. Aramo,[4] W. Benbow,[5] B. Bertucci,[3] E. Bissaldi,[6] J. H. Buckley,[7] M. Capasso,[8] D. Cerasole,[6] Z. Curtis-Ginsberg,[9] M. De Lucia,[10] L. Di Venere,[6] M. Escobar Godoy,[11] Q. Feng,[5] E. Fiandrini,[3] A. Furniss,[11] N. Giglietto,[6] F. Giordano,[6] R. Halliday,[12] W. Hanlon,[5] O. Hervet,[11] J. Hoang,[11] W. Jin,[1] D. Kieda,[13] N. La Palombara,[14] E. Leonora,[15] S. Loporchio,[6] G. Maier,[16] G. Marsella,[17] K. Meagher,[9] R. Mukherjee,[8] N. Otte,[18] R. Paoletti,[19] G. Pareschi,[20] N. Randazzo,[15] D. Ribeiro,[21] L. Riitano,[9] E. Roache,[5] L. Saha,[5] M. Santander,[1] R. Shang,[8,*] G. Tovmassian,[22] G. Tripodo,[17] V. V. Vassiliev,[23] J. J. Watson,[16] P. Yu[23] and A. Zink[24]

[1] *Department of Physics and Astronomy, University of Alabama, Tuscaloosa, AL 35487, USA*

[2] *Physics Department, Columbia University, New York, NY 10027, USA*

[3] *INFN Sezione di Perugia, 06123 Perugia, Italy*

[4] *INFN Sezione di Napoli, 80126 Napoli, Italy*

[5] *Center for Astrophysics | Harvard & Smithsonian, Cambridge, MA 02138, USA*

[6] *Dipartimento Interateneo di Fisica dell'Università e del Politecnico di Bari, 70126 Bari, Italy*

[7] *Department of Physics, Washington University, St. Louis, MO 63130, USA*

[8] *Department of Physics and Astronomy, Barnard College, Columbia University, NY 10027, USA*

[9] *Department of Physics and Wisconsin IceCube Particle Astrophysics Center, University of Wisconsin, Madison, WI 53706, USA*

[10] *INFN Sezione di Napoli, 80126 Napoli, Italy*

[11] *Santa Cruz Institute for Particle Physics and Department of Physics, University of California, Santa Cruz, CA 95064, USA*

[12] *Dept. of Physics, Elmhurst University, Chicago, IL 60126, USA*

[13] *Department of Physics and Astronomy, University of Utah, Salt Lake City, UT 84112, USA*

[14] *INAF - IASF Milano, 20133 Milano, Italy*

[15] *INFN, Sezione di Catania, Via Santa Sofia 64, Catania, 95123 Italy*

[16] *Deutsches Elektronen-Synchrotron, Platanenallee 6, 15738 Zeuthen, Germany*

[17] *Dipartimento di Fisica e Chimica "E. Segrè", Università degli Studi di Palermo, via delle Scienze, 90128 Palermo, Italy*

[18] *School of Physics & Center for Relativistic Astrophysics, Georgia Institute of Technology, Atlanta, GA 30332-0430, USA*

[19] *Dipartimento di Scienze Fisiche, della Terra e dell'Ambiente, Università degli Studi di Siena, 53100 Siena, Italy*

[20] *INAF - Osservatorio Astronomico di Brera, 20121 Milano/Merate, Italy*

[21] *School of Physics and Astronomy, University of Minnesota, Minneapolis, MN 55455, USA*

[22] *Instituto de Astronomía, Universidad Nacional Autónoma de México, Ciudad de México, Mexico*

PoS(ICRC2023)587

[23] *Department of Physics and Astronomy, University of California, Los Angeles, CA 90095, USA*
[24] *Friedrich-Alexander-Universität Erlangen-Nürnberg, Erlangen Centre for Astroparticle Physics, D 91058 Erlangen, Germany*

E-mail: r.y.shang@gmail.com

The Cherenkov Telescope Array (CTA) is the major next-generation ground-based observatory for studying the very-high-energy non-thermal Universe through gamma rays. The observatory will operate across a wide energy range from 30 GeV up to greater than 300 TeV with two observation sites in both hemispheres consisting of a variety of Large-, Medium-, and Small-sized Imaging Atmospheric Cherenkov Telescopes (IACT). The innovative Schwarzschild-Couder Telescope (SCT) is a candidate design and a proposed major U.S. contribution of a total of 11 Medium-sized, 9m aperture telescopes for CTA southern site. Based on the experience of the current generation IACT observatories, the SCT represents the perfection of IACT technology, being designed to simultaneously achieve a wide field of view and high imaging resolution by implementing novel, aspheric dual-mirror optics, and compact silicon photomultiplier detectors. The addition of 11 SCTs to CTA south will advance the science capabilities of CTA particularly for conducting sky surveys, resolving source confusions in populated regions, detecting multi-messenger transients with poorly known initial localization in follow-up observations, and delineating the morphology of gamma-ray sources with large angular extent. This presentation will provide an overview of the SCT optical system and the measurement of the optical performance. A simulation study, including the ability to resolve source confusion and extended source morphology measurement, to demonstrate the expected science performance improvement of CTA with SCTs will also be presented. This study is based on CTA Prod3b simulations with an SCT model dating back to 2016. The results will be updated with a new analysis chain that includes the forthcoming updated SCT model from Prod6 simulations. Furthermore, the event reconstruction used for this analysis is a straightforward extension of the analysis that was optimized for telescopes with larger pixels and coarser image resolution. Continuing improvements in the simulation model and analysis approach might present significant future changes.

The 38th International Cosmic Ray Conference
July 26–Aug 3, 2023
Nagoya, Japan

1. Introduction

Imaging Atmospheric Cherenkov Telescopes (IACTs) detects γ rays in the energy range from 80 GeV to above 100 TeV. The current generation IACT observatories have successfully detected > 50 Galactic accelerators. The majority of these Galactic sources are associated with SNRs and PWNe (pulsar wind nebulae). The next-generation observatory Cherenkov Telescope Array (CTA) is expected to discover more γ-ray emitting SNRs and PWNe through the Galactic Plane Survey (GPS) of its Key Science Projects (KSPs) [2], which is expected to be more sensitive than the current IACT observatories by a factor of $5-20$. The GPS will carry out a survey of the full Galactic plane with more concentrated coverage in the inner Galactic region of -60° to $+60^\circ$ in longitude.

Detecting PWNe and SNRs in the TeV regime provides valuable information about the high-energy processes that occur in these astrophysical objects, including the particle acceleration mechanisms and the properties of the magnetic fields in these objects. For example, SNR RX J1713.7-3946 is an established TeV gamma-ray emitter, however, the nature of its emission is still in debate. The ambiguity between leptonic v.s. hadronic origin of gamma-ray emission can be resolved by spectro-morphological analysis and comparison with the synchrotron X-ray emission and the CO material revealed in radio emission. The spectro-morphological analysis is not yet feasible for the data obtained by the current IACTs due to the lack of statistics at above 10 TeV and limited angular resolution, but CTA will be capable of such analysis. Indeed, a simulation study by [1] has demonstrated that CTA will be sensitive in differentiating the morphological features of leptonic v.s. hadronic emissions.

Resolving the small morphology features of the Galactic accelerators is a major challenge for CTA PeVatron KSP in addition to source confusion in the inner Galactic plane due to unknown morphology of sources, unknown level of diffuse emission, and high density of sources. The Schwarzschild-Couder telescope (SCT) is designed to maintain an optical PSF of 3.2 arcmin across a wide 8-degree FoV with its dual-mirror optics [4] and compact SiPM detector [7]. In this presentation, we will demonstrate that with the large FoV and excellent angular resolution, the additional 11 SCTs to the alpha CTA configuration will further improve CTA's ability in resolving source confusion, detecting small scale features and differentiating particle acceleration mechanisms inside Galactic accelerators.

2. Cherenkov Telescope Array and Schwarzschild-Couder Telescopes

Based on the success of the current IACT observatories and technonlgies, CTA aims to achieve a factor of 10 better sensitivity in detecting γ rays with more than 60 telescopes of three different types (Large-sized, Medium-sized, adn Small-sized), located in two observatories in both northern and southern hemispheres, to cover a wide energy range from 20 GeV to 300 TeV [2].

Most of the Galactic γ-ray sources detected and angularly resolved by the current generation IACTs are in the range of angular sizes between 0.1° and 1°. The lower limit of the angular size is constrained by the PSF, while the upper limit of the angular size is constrained by the field of view of the instruments.

The current generation of IACTs typically use the Davies-Cotton (DC) design, which consists of a single parabolic reflector. While the DC design has proven to be reliable for detecting atmospheric

Cherenkov light emissions, it is limited by spherical and comatic aberrations, which cause a small size of the field of view and a large camera plate scale. As a result, the DC design is constrained to the use of photomultiplier tubes (PMTs) as the photosensor technology, which have relatively low imaging resolution.

The prototype Schwarzschild-Couder telescope (pSCT), which has been constructed and commissioned at the Fred Lawrence Whipple Observatory in Arizona, USA, implements a design of aplanatic dual-mirror optics. The dual-mirror optics corrects spherical and comatic aberrations and de-magnifies the camera plate scale, allowing the use of silicon photomultipliers (SiPMs) for high-resolution cameras with highly integrated camera electronics [11]. The SCT technology provides a wide FoV of 8° and high imaging resolution of 0.067°, which can make an important impact on resolving source morphology in small angular scales (< 0.1°) as well as detecting extended sources in large angular scales (> 1.0°).

3. The optical and camera systems of SCT

The Schwarzschild-Couder optical system (OS) of the pSCT achieves full correction of spherical and comatic aberrations across the entire 8° field of view (FoV) through the use of a dual-mirror optical system, consisting of a primary mirror (M1) and a secondary mirror (M2), see Figure 1 (Top). The de-magnifying secondary mirror reduces the effective focal length of the OS, which enables the use of a high-resolution SiPM detector. The 9.7-m primary mirror is segmented into 48 panels, and the 5.4-m secondary mirror is segmented into 24 panels. Each panel is supported by a Stewart platform with six linear actuators which provide six degrees of freedom of the motion of the panels, whose relative position with respect to the neighboring panels is monitored by several mirror-panel edge sensors (MPESs).

As the first stage of the project, a camera equipped with 24 photosensor modules was installed in 2018. Each camera module will consist of 64 SiPM image pixels, each with a 6mm × 6mm photosensitive area. Each module has a front-end electronics unit containing the pre-amplifier, the digitization and the low-level trigger electronics. If the analog sum of the signals from four adjacent image pixels crosses a trigger threshold, a trigger pixel is generated. A camera trigger is further generated if a coincidence of three adjacent trigger pixels occurs. The camera trigger then initiates digitization and data read-out. In the final pSCT design, the camera will house 177 modules covering an 8° field of view with 11,328 SiPM pixels, see Figure 1 (Bottom). The full camera is expected to be installed and operating in 2024.

4. Simulation setup

The simulation results presented here were produced by the CTOOLS (version 2.0.0) software package [9]. The CTOOLS package has been developed for the analysis of the future CTA data as well as the current IACT observatories, including H.E.S.S., MAGIC, and VERITAS.

The simulated events are created with the CTOBSSIM tool. The CTOBSSIM tool uses the Instrument Response Functions (IRFs) that characterize the instrument performance and the input models that describe the source morphology and spectral information. The CTA IRFs also model

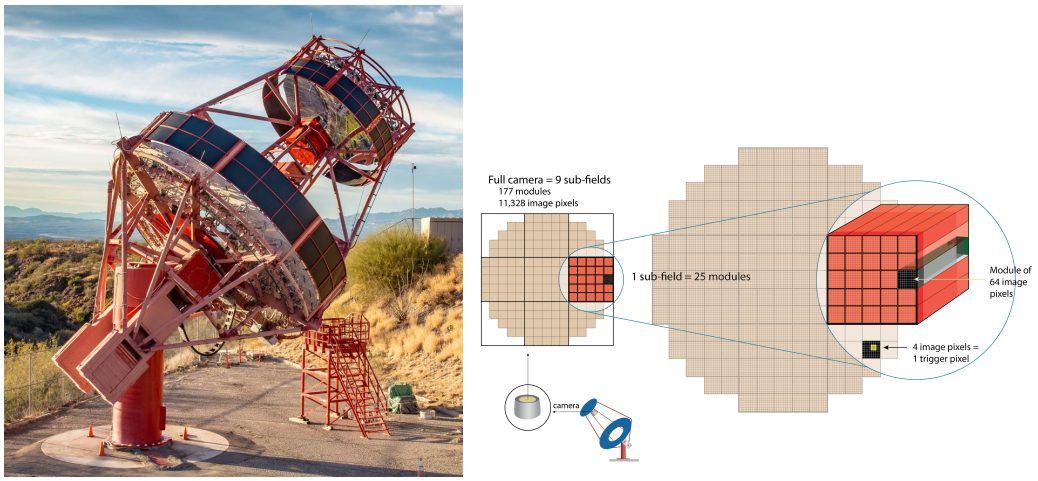

Figure 1: Left: The dual-mirror pSCT constructed at the Fred Lawrence Whipple Observatory in Arizona, USA. Right: The SiPM camera scheme of the pSCT.

the simulated background events, which are described by a function of position in the field of view and event energy.

The IRFs are derived from Monte Carlo (MC) simulations of CTA instrument [3] based on the CORSIKA air shower code [8] and telescope simulation tool sim_telarray [5]. The simulation results presented here use the IRF that assumes that the objects are observed at a zenith angle of 20° and that analysis cuts are optimized for a 50-hours observation. This research has made use of the CTA Simulation Telescope Models provided by CTA Observatory and Consortium (version prod3b v1.0; [6]).

5. Performance of resolving source confusion and source morphology

During the phase of initial commissioning of the pSCT in December 2019, an on-axis PSF of 2.8 arcmin has been achieved and led to a detection of the Crab nebula. The full alignment of the optical system across the 8-degree FoV was initially completed in 2022, and the measured PSF as function of the off-axis angle is shown in Figure 2 (Left).

Figure 2 (Right) demonstrates the improvement of the additional 11 SCTs to CTA in resolving sources with small extensions. A simulated γ-ray emission from Cas A placed at different distances is used to test the ability of detecting the source extension of the alpha CTA configuration of 14 MSTs (blue curve) v.s. the CTA configuration of 14 MSTs + 11 SCTs (black curve). The significance of the extended source detection is defined as

$$\Delta = \sqrt{\chi^2_{\text{point-source}} - \chi^2_{\text{extended-source}}}, \tag{1}$$

where $\chi^2_{\text{point-source}}$ is the goodness of fit using the instrument PSF and the point-source assumption, while $\chi^2_{\text{extended-source}}$ allows a non-zero source radius. The extended source is detected if $\Delta > 5$ as indicated by the red line. In a 2-hours observation, the 14 MSTs configuration is able to detect a source with an intrisic radius of 0.033° while the 14 MSTs + 11 SCTs configuration is able to detect a source with an intrisic radius of 0.015°.

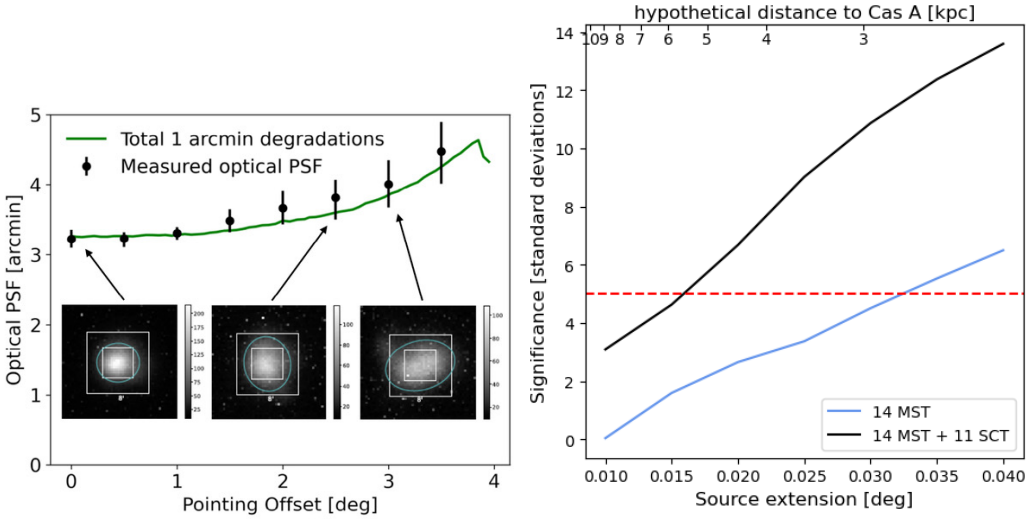

Figure 2: Left: The measurement of optical PSF of pSCT as function of off-axis angle. The PSF is maintained across the 8-degree FoV with a total of 1 arcmin degradation toward the edge. Right: The expected significance of detecting extended source as function of the true sources extension for the 14 MSTs configuration (blue curve) and for the 14 MSTs + 11 SCTs configuration (black curve) under a 2-hours observation. The source has a flux strength of 1% Crab unit.

We further demonstrate the ability in resolving source confusion using two simulated γ-ray sources separated by 0.2° in Figure 3. Both sources have γ-ray flux of 10% Crab Unit. Figure 3 (Top left) shows the image of the two sources observed by the 14 MSTs configuration, and Figure 3 (Top right) shows the the image of the two sources observed by the 14 MSTs + 11 SCTs configuration. These images are deconvolved using Richardson-Lucy Deconvolution algorithm with the PSFs derived from single point-source observations. The deconvolved images are shown in the bottom plots of Figure 3. In the case of the 14 MSTs configuration (Bottom left), the two sources are resolved into two separate sources, and yet the 14 MSTs + 11 SCTs configuration is able to improve the resolution and show a clear separation between the two sources.

The additional 11 SCTs can improve CTA's sensitivity in differentiating acceleration mechanisms inside the accelerators with high angular resolution γ-ray images that allow spectro-morphological analysis. Figure 4 (Top left) shows the simulated γ-ray image of RX J1713.7-3946 (generated from a template using the radio image of the SNR shell) at a distance of 1 kpc obtained with the 14 MSTs configuration, and Figure 4 (Top right) shows the image obtained with the 14 MSTs + 11 SCTs configuration. The image obtained with the 14 MSTs + 11 SCTs configuration shows more detailed structures of the SNR, this morphology information, together with the X-ray and radio observations, is critical for understanding the physics behind the γ-ray emission. A study using RX J1713.7-3946 as an example to differentiate leptonic v.s. hadronic emission mechanisms is presented by Laurel Carpenter.

The additional 11 SCTs will also improve CTA's ability in resolving extended sources at large distance. This is demonstrated in the two bottom images of Figure 4, where the simulation assumes that RX J1713.7-3946 was located at a distance of 3 kpc. While the 14 MSTs configuration can detect the 3-kpc source as an extended source, the 14 MSTs + 11 SCTs configuration can resolve

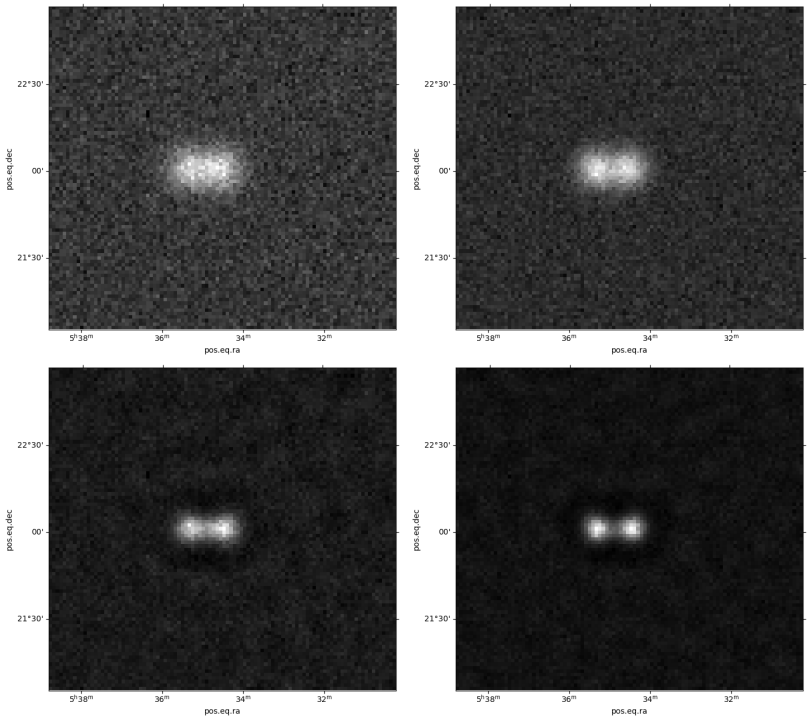

Figure 3: Top left: The image of the simulation of two point-like sources (each has a flux of 10% Crab unit) separated by 0.2 degrees obtained by the 14 MSTs configuration. Top right: The image of two point-like sources obtained by the 14 MSTs + 11 SCTs configuration. Bottom left: The image of two sources obtained by the 14 MSTs configuration after the deconvolution. Bottom right: The image of two sources obtained by the 14 MSTs + 11 SCTs configuration after the deconvolution.

the source with better morphology details and reveal the shell of the SNR.

6. Future work for pSCT

The pSCT is undergoing a major upgrade for its SiPM camera and front-end electronics. The camera was only equipped with one inner sector, which had successfully detected the Crab nebula. Now it will be populated with all 9 camera sectors (177 modules, 11328 pixels) and cover the whole 8-degree FoV. The camera electronics is being upgraded to reduce noise, these upgrades include using an integrated preamplifier (SMART ASIC) attached to the SiPM boards, an analog buffer with 16k cells per channel allowing 16 μs storage depth, and an adjustable trigger threshold for each group of 4 trigger pixels per ASIC. These upgrades will improve in single photon resolution, lower minimum threshold, and reduction of noise both on digitized signals and in the trigger circuit. The upgrade is currently expected to be completed in early 2024.

Acknowledgments

We gratefully acknowledge financial support from the agencies and organizations that can be found at this URL: https://www.cta-observatory.org/consortium_acknowledgments/. The research leading to these results has received funding from the European Union's Seventh Framework Programme (FP7/2007-2013) under grant agreements

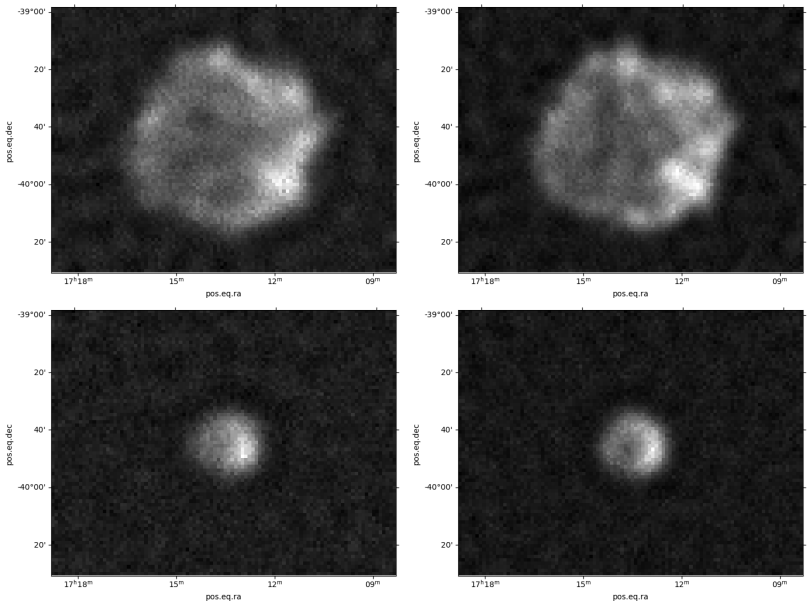

Figure 4: Top left: The simulated γ-ray image of RX J1713.7-3946 at a distance of 1 kpc obtained by the 14 MSTs configuration. Top right: The image of RX J1713.7-3946 at 1 kpc obtained by the 14 MSTs + 11 SCTs configuration. Bottom left: The image of RX J1713.7-3946 at a hypothetical distance of 3 kpc obtained by the 14 MSTs configuration. Bottom right: The image of RX J1713.7-3946 at 3 kpc obtained by the 14 MSTs + 11 SCTs configuration.

No 262053 and No 317446. This project is receiving funding from the European Union's Horizon 2020 research and innovation programs under agreement No 676134. We would like to thank the computing centres that provided resources for the generation of the Instrument Response Functions, see [10] for a complete list of the computing centres.

References

[1] Fabio Acero, Roberto Aloisio, J Amans, Elena Amato, Lucio Angelo Antonelli, Carla Aramo, T Armstrong, F Arqueros, Katsuaki Asano, Michael Ashley, et al. Prospects for Cherenkov Telescope Array Observations of the Young Supernova Remnant RX J1713. 7- 3946. *The Astrophysical Journal*, 840(2):74, 2017.

[2] Bannanje Sripathi Acharya, Iván Agudo, Imen Al Samarai, R Alfaro, J Alfaro, C Alispach, R Alves Batista, JP Amans, E Amato, G Ambrosi, et al. Science with the Cherenkov Telescope Array. 2017.

[3] A Acharyya, Iván Agudo, EO Angüner, Ruben Alfaro, J Alfaro, Cyril Alispach, Roberto Aloisio, R Alves Batista, J-P Amans, Lorenzo Amati, et al. Monte Carlo studies for the optimisation of the Cherenkov Telescope Array layout. *Astroparticle Physics*, 111:35–53, 2019.

[4] Colin Adams, Ruben Alfaro, Giovanni Ambrosi, Michelangelo Ambrosio, Carla Aramo, Wystan Benbow, Bruna Bertucci, Elisabetta Bissaldi, M Bitossi, Alfonso Boiano, et al. Verification of the optical system of the 9.7-m prototype Schwarzschild-Couder Telescope. In *Optical System Alignment, Tolerancing, and Verification XIII*, volume 11488, pages 10–28. SPIE, 2020.

[5] Konrad Bernlöhr. Simulation of imaging atmospheric Cherenkov telescopes with CORSIKA and sim_telarray. *Astroparticle Physics*, 30(3):149–158, 2008.

[6] Konrad Bernlöhr, Gernot Maier, and Abelardo Moralejo. CTAO Simulation Telescope Models for CORSIKA and sim_telarray -prod3b, February 2022.

[7] CTA SCT Consortium et al. Design and performance of the prototype Schwarzschild-Couder Telescope camera. *Proceedings of Science*, 395:748, 2022.

[8] Dieter Heck, Johannes Knapp, JN Capdevielle, G Schatz, and T Thouw. CORSIKA: A Monte Carlo Code to Simulate Extensive Air Showers. *Report FZKA 6019*, 1998.

[9] Jürgen Knödlseder, M Mayer, C Deil, J-B Cayrou, E Owen, N Kelley-Hoskins, C-C Lu, R Buehler, F Forest, T Louge, et al. GammaLib and ctools-a software framework for the analysis of astronomical gamma-ray data. *Astronomy & Astrophysics*, 593:A1, 2016.

[10] Gernot Maier. CTAO Instrument Response Functions - version prod3b-v2. https://zenodo.org/record/5163273.

[11] Vladimir Vassiliev, S Fegan, and P Brousseau. Wide field aplanatic two-mirror telescopes for ground-based γ-ray astronomy. *Astroparticle Physics*, 28(1):10–27, 2007.